

Link Adaptation of Precoded MIMO-OFDMA System with I/Q Interference

Udesh Oruthota and Olav Tirkkonen
 Department of Communications & Networking,
 Aalto University School of Science and Technology,
 P.O.Box 13000, FI-02150, Aalto, Finland.
 e-mail: `firstname.lastname@aalto.fi`

Abstract—This paper addresses achievable rates and related link adaptation for precoded multiple input multiple output transmission in an orthogonal frequency division multiple access system with uncompensated frequency flat transceiver I/Q imbalance. Precoder selection on the mirror subcarrier induces variations of the signal quality on the subcarrier of interest, and causes outage. We consider link adaptation strategies with infinite rate granularity for block and ergodic fading models where the transmitter knows the statistics of the induced interference, and has perfect channel state information of the wanted link. An optimal I/Q aware transmission method is used for these fading models. Performance of I/Q aware methods is compared with blind back-off selection.

Index Terms—MIMO-OFDMA, I/Q imbalance, outage capacity, link adaptation, precoding.

I. INTRODUCTION

Orthogonal Frequency Division Multiplexing (OFDM) and Orthogonal Frequency Division Multiple Access (OFDMA) are used in the Long Term Evolution (LTE) system of the 3rd Generation Partnership Project (3GPP) [1], and in IEEE 802.16 Worldwide Interoperability for Microwave Access (WiMax) [2]. Combined with Multiple-Input Multiple-Output (MIMO) technologies, OFDMA provides high spectral efficiency and multiuser diversity in frequency selective channels, especially when Channel State Information (CSI) is available at the transmitter [3]. With frequency-selective CSI, OFDMA may be fully scheduled, so that resources are flexibly allocated to different users in the frequency domain, see [3]–[5], and near optimal precoding MIMO techniques may be used [3]. In packet radios, link adaptation with Adaptive Modulation and Coding (AMC) [6] is used to tune the transmission rate to the instantaneous channel quality. Indeed, downlink LTE is based on precoding MIMO with frequency-selective feedback, and link adaptation is performed in the frequency, spatial directivity and spatial rank domains [7]. Future Fifth generation systems are likely to share many of these properties with LTE and WiMax [8].

The direct-conversion architecture is an attractive solution for low-cost, low-power, and small-size communication transceivers due to its implementation simplicity. However, when higher order modulation is applied to achieve a high data rates, imperfections in Radio Frequency (RF) front-ends start to restrict the communication quality. One such is the I/Q imbalance, caused by an amplitude and phase mismatch

between the I (in-phase) and Q (quadrature-phase) branches in the quadrature (de)modulators. The effects of other RF impairments, such as phase noise and frequency offset, can be mitigated by a suitable parametrization of the modulation scheme [8]. As this does not hold for I/Q imbalance, we concentrate on it in this paper.

I/Q imbalance in OFDM systems causes interference between a pair of mirror subcarriers, which are symmetric around the center subcarrier [9], [10]. The distortion caused by the I/Q imbalance may be compensated by jointly detecting the signals transmitted on two carriers which are mirror to each other [11]–[13]. Blind estimation of I/Q imbalance has been discussed in [14]–[16]. The effect of I/Q imbalance on MIMO-OFDM has been studied in [17], [18]. An I/Q imbalance correction scheme for OFDMA uplink has been addressed in [19], based on orthogonal pilot structure within the time-frequency resource block. Mitigation of inter-user interference in an OFDMA system with transmitter I/Q imbalance has been proposed in [20], based on joint channel equalization and multiuser detection.

In practice, the increased signal processing for I/Q compensation may not be cost-effective in some cases when comparing to the achievable gain. Hence, it is worthwhile to study the performance of a given system with the I/Q imbalance uncompensated at the signal detection.

When precoding is used in MIMO-OFDM, I/Q imbalance limits the precoding gains [21], [22]. Optimally, to compensate for the I/Q imbalance, the precoders on a carrier and its mirror should be jointly selected [22], [23]. If precoding is not jointly optimized in precoded MIMO-OFDM(A), changes in the precoding on a carrier causes non-controlled variation in the Signal-to-Interference-plus-Noise Ratio (SINR) experienced by the interference victim on the mirror carrier, due to the I/Q imbalance. This may cause mispredictions of the channel quality, wrong link adaptation decisions, and accordingly losses of transmissions.

Effects on link adaptation caused by variability of SINR due to channel estimation errors and feedback delays have been studied in [24]–[26]. In the context of precoded MIMO in a multicellular system, the so-called “Flashlight effect” has been discussed [27]–[29], where SINR varies due to interferer precoding change. To properly select a transmission mode in a situation with SINR variability, it is essential to know the SINR statistics. Optimal link adaptation for channel

quality misprediction due to time selective fading has been addressed in [26], and jointly for time selective fading, channel estimation errors and the flashlight effect in [29].

In [24]–[29], link adaptation with a finite set of modulation and coding schemes was considered. If one assumes a link adaptation scheme with an infinite granularity of ideal modulation and coding schemes [6], link adaptation amounts to knowing the pertinent capacity of the link, subject to fading according to the SINR statistics.

Link capacity has been addressed for a few channels with I/Q imbalance. For an OFDM-system with uncompensated I/Q imbalance, the ergodic capacity and outage probability was calculated in [30]. A single-carrier MIMO system with transmit beamforming was addressed in [18]. The ergodic capacity of an Multiple-Input-Single-Output (MISO) OFDM-system with antenna selection was derived in [31], and the outage probability for MISO-OFDM with transmit beamforming in [21]. To the best of our understanding, ergodic or outage capacity for precoded multistream MIMO-OFDMA systems with I/Q imbalance has not been addressed in the literature.

In this paper we study the distribution of uncompensated I/Q interference, and the related distribution of SINR in a precoded downlink MIMO-OFDMA system. We calculate the ergodic and outage capacities in the presence of I/Q interference, and use these for link-adaptation in an ideal system with an infinite granularity of modulation and coding schemes. Both the transmitters and receivers have perfect CSI of the channels carrying wanted signals.

The remainder of this paper is organized as follows. Section II presents a simplified system model. In Section III we identify the problem caused by the I/Q flashlight effect. Section IV introduces I/Q aware optimum link adaptation. Distributions of received SINR for a downlink transmission under block and ergodic fading channel models are derived, and performance is reported. In Section V, comparisons to a conservative blind back-off algorithm are shown, and in Section VI, system simulation results are provided. Section VII discusses the communication scenarios where the observed phenomena are relevant.

Notation. We use boldface upper and lower case letters to denote matrices and vectors, respectively. $(\cdot)^*$, $(\cdot)^T$ and $(\cdot)^H$, respectively represents complex conjugate, transpose and Hermitian conjugate. The Euclidean norm of vector is given by $\|\mathbf{x}\| = \sqrt{\mathbf{x}^H \mathbf{x}}$ and absolute value of x is denoted as $|x|$. The trace of the matrix \mathbf{X} is given by $\text{Tr } \mathbf{X}$. The identity matrix is denoted by \mathbf{I} , and specifically in m dimensions, by \mathbf{I}_m . The statistical expectation w.r.t x is represent by $\mathbb{E}_x\{\cdot\}$, and $f_X(x)$ and $F_X(x)$ are the probability density function and the cumulative distribution function of random variable x . The probability of an event is $P(\cdot)$.

II. SYSTEM MODEL

A. I/Q imbalance in MIMO-OFDMA system

We consider a time and frequency synchronized multiuser MIMO-OFDMA system with multiple data streams per user, as depicted in Fig. 1. The base station is equipped with N_T transmit antennas, and each user contains N_R receive

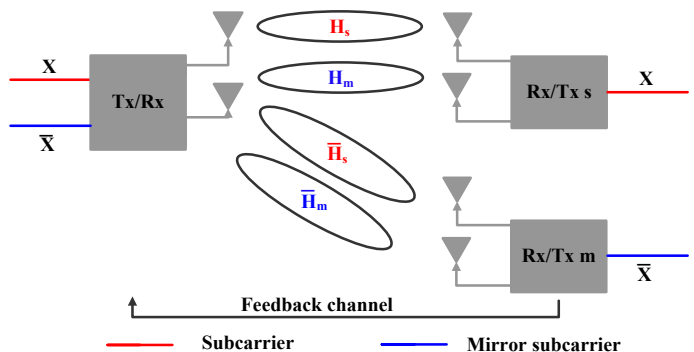


Fig. 1: System model for MIMO-OFDMA system on a mirror carrier pair. Channels on subcarrier s and its mirror subcarrier m are depicted, with wanted channels \mathbf{H}_s , $\bar{\mathbf{H}}_m$ and interfering channels \mathbf{H}_m , $\bar{\mathbf{H}}_s$.

antennas. Individual users are assigned a block of orthogonal subcarriers depending on their demands. The length of the Cyclic Prefix (CP) is assumed sufficiently large to overcome multipath fading effects.

All transmission chains experience a similar frequency flat I/Q imbalance. In an OFDM system, the I/Q imbalance couples the transmissions on two mirror carriers [9], [10]. Accordingly, our analysis can be restricted to a single mirror carrier pair. In a practical region of hardware operation, the I/Q imbalance is small [32], and can be modeled by small perturbations of the signals. If t_s is the transmitted signal before I/Q imbalance on the subcarrier s of interest, and t_m on its mirror carrier, the effect of transmitter I/Q imbalance is to add $\epsilon_T^* t_m^*$ to t_s before transmission. Similarly, if y_s is the received signal before I/Q imbalance on subcarrier s , and y_m on its mirror carrier, the effect of receiver I/Q imbalance is to add $\epsilon_R^* y_m^*$ to y_s before down converting to baseband. Here, $\epsilon_{T/R}$ are small complex numbers characterizing the phase and amplitude mismatches of the transmitter and receiver, respectively. The severity of the I/Q imbalance is quantified by an Image Rejection Ratio $\text{IRR} \approx 1/|\epsilon|^2$, separately for the transmitter and receiver.

For multiple access, subcarrier s is assigned to user s , and subcarrier m to user m . Four channel matrices are involved in the OFDMA transmission restricted to a mirror carrier pair, as illustrated in Fig. 1. Note that the same model with four channels holds for both uplink and downlink. The wanted signal channel matrix on subcarrier s between the base station and receiver s is \mathbf{H}_s and the corresponding interference channel on the mirror subcarrier is \mathbf{H}_m . Similarly there are two channel matrices for the user scheduled on subcarrier m , the interference channel $\bar{\mathbf{H}}_s$ on subcarrier s and the wanted signal channel $\bar{\mathbf{H}}_m$ on subcarrier m .

Precoding is applied at the multiantenna transmitters. On the subcarrier s of interest the rank- p precoder $\mathbf{W} \in \mathbb{C}^{M_T \times p}$ is used, and on the mirror m the rank- q precoder $\bar{\mathbf{W}} \in \mathbb{C}^{M_T \times q}$ is used. The precoders are normalized as $\text{Tr } \mathbf{W}^H \mathbf{W} = p$, and $\text{Tr } \bar{\mathbf{W}}^H \bar{\mathbf{W}} = q$. The transmit symbol vector on subcarrier s is $\mathbf{x} \in \mathbb{C}^{p \times 1}$ and the symbol vector on m is $\bar{\mathbf{x}} \in \mathbb{C}^{q \times 1}$. Symbols are drawn from a complex Gaussian symbol constellation with power constraint, $\mathbb{E}_{\mathbf{x}}\{\mathbf{x}\mathbf{x}^H\} = \frac{1}{\kappa} \mathbf{I}_\kappa$, $\kappa = p, q$.

In downlink, the I/Q corrupted $M_R \times 1$ received signal vector on the subcarrier of interest for s then becomes

$$\mathbf{y} = \mathbf{H}_s \mathbf{W} \mathbf{x} + (\epsilon_T^* \mathbf{H}_s + \epsilon_R \mathbf{H}_m^*) \overline{\mathbf{W}}^* \overline{\mathbf{x}}^* + \mathbf{n}_s + \epsilon_R \mathbf{n}_m^* \quad (1)$$

where \mathbf{n}_s and \mathbf{n}_m are the $\mathbb{C}^{M_R \times 1}$ Additive White Gaussian Noise (AWGN) noise vectors on mirror subcarriers with independent and identically distributed (i.i.d) $\mathcal{CN}(0, N_0)$ samples. As $|\epsilon_R \epsilon_T| \ll 1$ we have neglected a second order I/Q interference term. In (1), the desired signal is corrupted by the mirror symbol interference due to the transmitter and the receiver I/Q imbalance, as well as AWGN and its I/Q induced mirror reflection.

The covariance of the interference-plus noise disturbing the transmission on the subcarrier of interest is thus

$$\mathbf{C} = (\epsilon_T^* \mathbf{H}_s + \epsilon_R \mathbf{H}_m^*) \overline{\mathbf{W}}^* \overline{\mathbf{W}}^H (\epsilon_T \mathbf{H}_s^H + \epsilon_R^* \mathbf{H}_m^T) + (1 + |\epsilon_R|^2) \mathbf{I} \quad (2)$$

With I/Q blind precoding, the difference between OFDM and downlink OFDMA is that in OFDM, receive I/Q interference is precoded according to the channel that it is propagating over, $\overline{\mathbf{W}} = \overline{\mathbf{W}}(\mathbf{H}_m)$, whereas in downlink OFDMA, it is precoded according to an uncorrelated channel of another user, $\overline{\mathbf{W}} = \overline{\mathbf{W}}(\overline{\mathbf{H}}_m)$.

In uplink OFDMA, the channel dependency of the I/Q interference term in (1) would be given by the matrix $\epsilon_T^* \overline{\mathbf{H}}_s + \epsilon_R \overline{\mathbf{H}}_m$, and $\overline{\mathbf{W}} = \overline{\mathbf{W}}(\overline{\mathbf{H}}_m)$. Thus also for uplink OFDMA, receive I/Q interference would be precoded according to the channel it propagates over. Below we will concentrate on downlink OFDMA.

B. Strategies to Deal with I/Q Interference

Many strategies with different levels of complexity exist for dealing with the problem of I/Q induced interference in a MIMO-OFDM(A) system. In decreasing order of complexity, these would be

- a) Joint mirror-pair precoding for downlink transmissions [22], [23]. The precoders \mathbf{W} on subcarrier s and $\overline{\mathbf{W}}$ on subcarrier m are jointly selected, to maximize transmission rates to both users. For this, all four channels $\mathbf{H}_s, \mathbf{H}_m, \overline{\mathbf{H}}_s, \overline{\mathbf{H}}_m$ need to be known at the transmitter and receiver.
- b) Joint open-loop transmission [33], [34]. The transmissions on s and m are designed to yield full diversity both over the own subcarrier channels, and the I/Q interference channels. This requires joint decoding of the signals on s and m , requiring all four channels to be known at the receiver. This is best suited for situations where the receiver on these subcarriers are the same.
- c) I/Q compensation at the receiver [12], [17]. The receiver estimates the interference-plus-noise covariance \mathbf{C} , as well as the wanted channel \mathbf{H}_s . A minimum mean square error filter is used at the receiver to mitigate the interference. Alternatively, an optimum non-linear receiver may be used. For precoding, the transmitter needs information of \mathbf{H}_s .
- d) I/Q blind receiver. The receiver knows \mathbf{H}_s and uses it for linear eigenbeam reception. For precoding, the transmitter needs information of \mathbf{H}_s .

In this paper, we shall concentrate on strategies c) and d). With these receiver strategies, we analyze link-adaptation, where the transmission rate is optimized based on I/Q awareness, i.e. on knowledge of the *statistics* of the I/Q interference.

As we are interested in precoded multistream MIMO transmissions, we may consider joint Transmission (Tx) of codewords across all beams, or separate Tx for each beam. We shall use these in conjunction of Reception (Rx) strategies c) and d) as three Transmission-Reception (Tx-Rx) schemes:

- 1) Joint Tx-Rx: A codeword is jointly transmitted over all eigenbeams. Optimum non-linear MIMO reception is applied at Rx, based on estimated knowledge of the realized \mathbf{C} . The receiver is I/Q compensating in the sense of Strategy c).
- 2) Joint Tx-Separate Rx: A codeword is jointly transmitted over all eigenbeams. Linear per eigenbeam symbol detection is applied at Rx.
- 3) Separate Tx-Rx: Separate codewords are transmitted over the eigenbeams, and linear per eigenbeam detection is applied.

Schemes 2) and 3) thus apply I/Q blind reception. Scheme 3) is related to LTE, as there, the primary MIMO transmission method is transmit two codewords on separate MIMO layers.

C. Estimating Channels and Parameters

For all schemes, we apply the following *CSI and channel assumptions*. We assume that the frequency separation between mirror carriers is large compared to the coherence bandwidth of the system, so the mirror carriers are assumed to be independently fading, and that all channels $\mathbf{H} \in \mathbb{C}^{N_R \times N_T}$ contain i.i.d $\mathcal{CN}(0, 1)$ entries. We assume perfect instantaneous CSI of the subcarrier-specific wanted channels \mathbf{H}_s . For the joint reception scheme 1), the realized interference-plus-noise covariance \mathbf{C} is assumed perfectly known at the receiver. For separate transmission, unitary precoding is applied, as optimum power allocation is not analytically tractable. Further, frequency dispersion is mild enough so that channels are considered constant between measurement and transmission. Time dispersion is assumed to be mild enough so that the CP removes Inter-Symbol Interference (ISI).

Subject to assumptions on slow changes in channels, these assumptions can be realized by arranging orthogonal pilot transmission on s and m . Orthogonal pilots enable estimation of the wanted channels \mathbf{H}_s and $\overline{\mathbf{H}}_m$ without I/Q interference, and estimation of the I/Q parameters $\epsilon_{R/T}$ [19], [35], [36].

III. THE I/Q FLASHLIGHT EFFECT

A. Precoding Transmitter and Receiver

As in [3], we do not consider in-cell multiuser MIMO. There is a single user transmission per subcarrier. The minimal Singular Value Decomposition (SVD) of the wanted channel is $\mathbf{H}_s = \mathbf{U} \mathbf{\Sigma} \mathbf{V}^H$. With $N_{\min} = \min(N_T, N_R)$, the unitary left eigenbeam matrix \mathbf{U} is $N_R \times N_{\min}$ dimensional, the unitary right eigenbeam matrix \mathbf{V} is $N_T \times N_{\min}$, and the diagonal matrix $\mathbf{\Sigma}$ with singular values is $N_{\min} \times N_{\min}$.

With perfect CSI of the wanted channel, and no CSI about the instantaneous interference channels \mathbf{H}_m and $\overline{\mathbf{H}}_s$, the

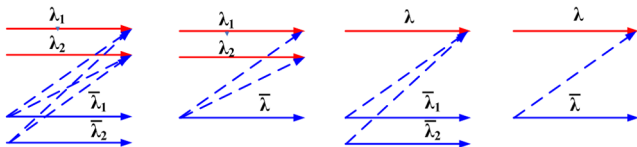


Fig. 2: Four interference situations in 2×2 MIMO, depending on the number of interfering eigenbeams transmitted on the mirror, and the number of victim eigenbeams on the subcarrier.

problem at transmission is to find a precoder for unknown noise covariance \mathbf{C} . It is straight forward to show that an optimum precoder \mathbf{W} lies in the column space of \mathbf{V} . Thus, without loss of generality, the optimal precoder is $\mathbf{W} = \mathbf{P}^{\frac{1}{2}} \mathbf{V}$, where \mathbf{P} is the diagonal power allocation matrix.

Each receiver attempts to detect only the symbols of their own transmissions. Interfering signals coming from I/Q imbalance are treated as noise. The Joint Tx-Rx scheme requires numerical analysis. For the schemes with separate reception, post-processing SINRs can be calculated. The received signal is multiplied with the left eigen matrix to yield $\hat{\mathbf{x}} = \mathbf{U}^H \mathbf{y}$, and the estimated signal of receiver s becomes

$$\hat{\mathbf{x}} = \Sigma \mathbf{x} + (\epsilon_T^* \Sigma \mathbf{V}^H + \epsilon_R \mathbf{U}^H \mathbf{H}_m^*) \bar{\mathbf{W}}^* \bar{\mathbf{x}}^* + \mathbf{U}^H (\mathbf{n}_s + \epsilon_R \mathbf{n}_m^*). \quad (3)$$

The post processing SINR of the k th eigenbeam then is

$$\gamma_k = \frac{p_k \lambda_k}{\left\| \left(\epsilon_T^* \sqrt{\lambda_k} (\mathbf{v}_k)^H + \epsilon_R (\mathbf{u}_k)^H \mathbf{H}_m^* \right) \bar{\mathbf{W}}^* \right\|^2 + \frac{(1 + \epsilon_R^2)}{\gamma_0}}. \quad (4)$$

Here λ_k is the k th eigenvalue of the channel \mathbf{H}_s , and \mathbf{u}_k and \mathbf{v}_k denote the k th eigenvector of the left and right unitary matrices \mathbf{U} and \mathbf{V} , respectively. The power allocation on eigenbeam k is given by p_k which represents the k th element of \mathbf{P} . The average Signal-to-Noise Ratio (SNR) is γ_0 .

In (4), the impact of the mirror precoder $\bar{\mathbf{W}}$ is clearly visible. If the mirror transmission applies a full-rank unitary precoder, the SINR does not depend on the mirror precoder $\bar{\mathbf{W}}$. Otherwise, both the a priori unknown I/Q channels, and the precoding, affect the interference. There is an *I/Q flashlight effect*.

Furthermore, from (4) it follows that if $\bar{\mathbf{W}}$ comes from a non-unitary, or non-full-rank ensemble, there is a *negative correlation* between the SINRs γ_k of different eigenbeams—the transceiver I/Q interference caused by the mirror transmission become a resource that is orthogonally shared among the eigenbeams k .

B. I/Q Interference Variability: A Motivating Example

Depending on the transmission ranks of the transmissions on the mirror subcarrier pair, different interference situations appear. For example, in a 2×2 MIMO system, four cases can be observed, depending on the number of eigenbeams on each subcarrier, as shown in Fig. 2. For rank one interference, we have spatially colored interference. With unitary precoding on

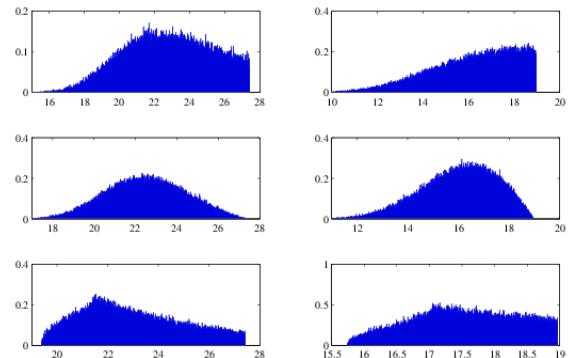


Fig. 3: Simulated probability density of SINR [dB] in a 2×2 system. First row: rank one interference according to (5). Second row: rank two interference (4). In both, wanted channel \mathbf{H}_s randomly distributed. Third row: One instance with fixed \mathbf{H}_s , rank one interference (5). Left: stronger eigenbeam, right: weaker eigenbeam.

subcarrier s of interest we then have

$$\gamma_k = \frac{\frac{1}{2} \lambda_k}{\left| \epsilon_R \mathbf{u}_k^H \mathbf{H}_m^* \bar{\mathbf{w}}^* + \epsilon_T^* \sqrt{\lambda_k} \mathbf{v}_k^H \bar{\mathbf{w}}^* \right|^2 + \frac{(1 + \epsilon_R^2)}{\gamma_0}}. \quad (5)$$

Although eigen beamforming is performed with perfect CSI at the transmitter, the I/Q interference varies depending on the mirror interference channel \mathbf{H}_m , and the user scheduled on the mirror subcarrier and its precoder $\bar{\mathbf{w}}$. This causes large fluctuations on the SINR observed at the receiver, as shown in Fig. 3 for SNR=IRR=25dB and unitary precoding. For an example fixed channel realization, in the third row of Fig. 3, we observe a variation of 8dB in the SINR, depending on the mirror precoder, and the mirror subcarrier channel.

Similar uncontrolled variability in interference is caused by beamforming transmissions in multicellular systems. In [28] it was argued that the effects of such interference variability were insignificant—partly they were overshadowed by other non-idealities of the system, such as the finite granularity in Channel Quality Indication (CQI) reporting, and channel estimation errors, partly they were mitigated by the retransmission protocols and open-loop link adaptation. Interestingly, the a priori weak interference caused by I/Q interference may have more damaging effects on MIMO-OFDMA system performance. MIMO provides gain at high SNR, where I/Q interference is noticeable. Compared to the variability caused by other cell beamforming [29], the variability caused by I/Q interference, as depicted in Fig. 3, is significantly wider. Accordingly, the protocols and system characteristics discussed in [28] are not sufficient to render the I/Q flashlight effect insignificant.

IV. I/Q AWARE LINK ADAPTATION

In OFDM based systems such as 3GPP LTE, scheduling in both time and frequency domains is possible [4], [5], [37]. We consider ergodic and block fading channel models that reflect two different scheduling strategies.

Depending on the channel model, interference variability either induces *fading* inside a coding block, or *outage* if the interference realization renders the channel worse than expected at transmission. With the I/Q flashlight effect, this happens *despite perfect CSI at transmitter and receiver* of the wanted channel \mathbf{H}_s . If the characteristics of the process causing outage or fading are not known when selecting the transmission scheme, packet losses or unexpected outage rates may occur. To optimize the selection of transmission rate, *I/Q aware link adaptation* may be considered.

For I/Q-aware estimation of the achievable transmission rates at the receiver, the characteristics of the SINR distribution have to be estimated. We assume that the receiver has Channel Distribution Information (CDI) of the interfering channels \mathbf{H}_m and $\bar{\mathbf{H}}_s$, or corresponding information of the interference-plus-noise covariance or SINR distributions. The transmission rate is recommended by the receiver to the transmitter by infinite granularity CQI feedback which corresponds to an infinite granularity ideal AMC scheme. CQI is based on the channel capacity, or achievable mutual information. Performance of an infinite granularity CQI scheme is indicative of performance with a discrete AMC set [6]. The mobile station provides CQIs for all possible ranks of the mirror transmission, or otherwise knows the rank of the mirror transmission. To estimate the CDI, one may either collect statistics from multiple measurements, or directly estimate the I/Q parameters.

A. Interference Statistics

For I/Q aware link adaptation, the distribution of the noise plus interference covariance \mathbf{C} , or the distribution of the interference terms in the SINRs γ_k have to be known. We mainly focus on the case when the I/Q interference has rank one, when the interference variability is largest. For concreteness, we concentrate on i.i.d. 2×2 MIMO channels, which allow closed form interference statistics.

First we investigate the distributions of some inner products. Consider the inner product between two unit-norm vectors \mathbf{v} and \mathbf{w} . The vectors are uniformly distributed over Grassmanian spaces. These are homogeneous spaces of unitary groups, and they inherit an invariant measure from the invariant Haar measure of the groups. The probability measure of these vectors is invariant under the rotation by a unitary matrix. The distribution of $|\mathbf{v}^H \mathbf{w}|^2$ then equals the distribution of the absolute value squared of an element of a unit norm vector. For two eigenbeams, the distribution of $|\mathbf{v}^H \mathbf{w}|$ is uniform in $[0, 1]$.

Next, consider the Random Variable (RV) $\mathbf{u}^H \mathbf{H} \mathbf{w}$, where \mathbf{u} and \mathbf{w} are arbitrary unit norm vectors, and \mathbf{H} is a random matrix with i.i.d Gaussian $\mathcal{CN}(0, 1)$ entries. As a normed linear combination of complex Gaussian RVs, this RV is also $\mathcal{CN}(0, 1)$.

From (5), the distribution of SINRs are determined by the distribution of I/Q interference plus noise. We first analyze the interference power distribution. For simplicity we omit the subscript k of the eigenbeam. For a known wanted channel \mathbf{H}_s , the I/Q interference in (5) can be written as

$$I = \epsilon_T^* \sqrt{\lambda} \mathbf{v}^H \bar{\mathbf{w}}^* + \epsilon_R \mathbf{u}^H \mathbf{H}_m^* \bar{\mathbf{w}}^* = \epsilon_T^* e^{j\theta} \sqrt{\lambda} \alpha + \epsilon_R h, \quad (6)$$

where $\mathbf{v}^H \bar{\mathbf{w}}^* = \alpha e^{j\theta}$ and $\mathbf{u}^H \mathbf{H}_m^* \bar{\mathbf{w}}^* = h$. From the analysis above it follows that $f(\alpha) = 2\alpha$, and h is i.i.d $\mathcal{CN}(0, 1)$. Now, the I/Q interference can be modelled as a Rician distribution.¹ The power of the Line-of-Sight (LOS) component is $s^2 = (\alpha \epsilon_T)^2 \lambda$ and the average power of the scattered components is $2\sigma^2 = \epsilon_R^2$. The distribution of the I/Q interference power thus follows the Rician power distribution, and

$$f_I(i | \mathbf{H}_s, \alpha) = \frac{1}{\epsilon_R^2} e^{-\frac{\epsilon_T^2 \lambda \alpha^2 + i}{\epsilon_R^2}} I_0 \left(\frac{2\sqrt{i\lambda\alpha}}{\epsilon_R/\epsilon_T} \right) \quad (7)$$

where $I_0(z)$ is the modified Bessel function of first kind. To obtain the I/Q interference power distribution $f_I(i | \mathbf{H}_s)$, we have to average over the distribution of α . The modified Bessel function can be represented as an infinite series $I_0(z) = \sum_{m=0}^{\infty} \frac{1}{(m!)^2} \left(\frac{z}{2}\right)^{2m}$, resulting in

$$f_I(i | \mathbf{H}_s) = e^{-\frac{i}{\epsilon_R^2}} \sum_{m=0}^{\infty} \frac{1}{(m!)^2} \frac{i^m}{\lambda \epsilon_T^2 \epsilon_R^{2m}} \Gamma \left[m + 1, \frac{\epsilon_T^2 \lambda}{\epsilon_R^2} \right] \quad (8)$$

Here, $\Gamma[a, b] = \int_0^b t^{a-1} e^{-t} dt$ is the incomplete Gamma function.

For rank-two transmission with rank-one interference, $\sum_{k=1}^2 |(\mathbf{v}_k)^H \bar{\mathbf{w}}^*|^2 = 1$ so that $\alpha_2 = \sqrt{1 - \alpha_1^2}$. The I/Q interference on the two eigen directions are correlated. The joint interference power distribution is then

$$\begin{aligned} f_{I_1, I_2}(i_1, i_2 | \mathbf{H}_s) &= \int_0^1 f_I(i_1 | \mathbf{H}_s, \alpha) f_I(i_2 | \mathbf{H}_s, \sqrt{1 - \alpha^2}) 2\alpha d\alpha \\ &= \frac{e^{-i_1 - i_2 - \tilde{\lambda}_2}}{\epsilon_R^4} \sum_{m=0}^{\infty} \sum_{n=0}^{\infty} \frac{\tilde{i}_1^m \tilde{i}_2^n \tilde{\lambda}_1^m \tilde{\lambda}_2^n}{m!^2 n!^2} \\ &\quad \times \mathcal{M}(m + 1, m + n + 2, \tilde{\lambda}_2 - \tilde{\lambda}_1) \end{aligned} \quad (9)$$

where $\mathcal{M}(a, b, z) = \int_0^1 e^{zu} u^{a-1} (1 - u)^{b-a-1} du$ is $\Gamma[a]\Gamma[b - a]/\Gamma[b]$ times Kummer's confluent Hypergeometric function and $\Gamma[x] = (x - 1)!$ is the gamma function. Scaled variables $\tilde{i}_k = i_k/\epsilon_R^2$ and $\tilde{\lambda}_k = \lambda_k \epsilon_T^2/\epsilon_R^2$ have been used.

B. Block Fading Channels

First, assume that the transmitter allocates resources such that a coding block is transmitted within the coherence bandwidth and coherence time of the channel, so that the channel inside the code block is both frequency and time flat. Such a transmission can thus be modeled as a block fading channel. The channel gains are assumed constant within the code block and change independently from block to block. Encoding over one fading realization is considered. Scheduling decisions are based on knowing each channel realization on the subcarrier of interest.

The corresponding channel used for communication on a subcarrier, or on a collection of subcarriers within the coherence bandwidth, can be formalized as a *block fading I/Q flashlight channel*, where \mathbf{H}_s is fixed, and the interference-plus-noise covariance \mathbf{C} varies. The channel is characterized by the statistic $f_C(\mathbf{C})$, which is related to the statistics of the

¹The Rician distribution is given by $p(x) = \frac{x}{\sigma^2} \exp\left\{-\frac{x^2 + s^2}{2\sigma^2}\right\} I_0\left(\frac{x s}{\sigma^2}\right)$ with the $K = s^2/2\sigma^2$ where s^2 is the power of the LOS component and $2\sigma^2$ is the power of the scattered components.

underlying variables \mathbf{H}_m and $\bar{\mathbf{W}}$. This is a fading channel with unboundedly deep fades caused by the unknown \mathbf{H}_m and $\bar{\mathbf{W}}$.

CQI is based on calculating the mutual information of this channel, depending on the Tx-Rx strategy, and maximizing the rate R for an outage probability P_{out} . For practical purposes, the *throughput* $(1 - P_{\text{out}})R$ is of interest, and the *expected throughput* at a given outage probability is obtained by averaging $(1 - P_{\text{out}})R$ over \mathbf{H}_s . The *maximum throughput* is obtained by maximizing over P_{out} . The CQI is a recommendation of the transmitter to use such a rate. For separate transmission, this optimization would be performed per beam.

1) *Joint Tx-Rx*: The receiver knows the instantaneous realization of \mathbf{C} and \mathbf{H}_s , as well as $f_C(\mathbf{C})$. The transmitter knows \mathbf{H}_s . Optimum joint reception of the MIMO transmission is performed. The optimum transmission method, subject to this CSI, achieves the *outage capacity* of this channel. Given a transmission covariance $\mathbf{Q} = \mathbf{W}\mathbf{P}\mathbf{W}^H$ and the CSI, the mutual information is given by $M = \log_2 \{ \det [\mathbf{I} + \mathbf{H}_s \mathbf{Q} \mathbf{H}_s^H \mathbf{C}^{-1}] \}$. Given an outage probability P_{out} and the CDI, a transmission rate $R(P_{\text{out}} | \mathbf{Q}, \mathbf{H}_s)$ can then be selected from the known distribution of mutual information $f_M(M | \mathbf{Q}, \mathbf{H}_s)$. By selecting the best transmission covariance, the outage capacity R for P_{out} is found for the channel with fixed \mathbf{H}_s .

Now consider rank-two transmission with unitary precoding. Conditioned on a given channel matrix \mathbf{H}_s and inner product α , the I/Q interference on the two eigenbeams $\mathbf{i} = [i_1 \ i_2]^T$ contains Rician distributed elements, and the I/Q interference vector can be represented as $\mathbf{i} = \mathbf{m} + \mathbf{i}_w$ where $\mathbf{m} = \mathbb{E}\{\mathbf{i}\} = [\epsilon_T^* e^{j\theta_1} \sqrt{\lambda_1} \alpha, \ \epsilon_T^* e^{j\theta_2} \sqrt{\lambda_2} (1 - \alpha^2)]^T$, and \mathbf{i}_w is a vector of i.i.d complex Gaussian entries. Then the distribution of I/Q interference covariance $f_C(\mathbf{C} | \mathbf{H}_s, \alpha)$ can be modeled as a non-central Wishart distribution $\mathbf{W}(2, \mathbf{\Upsilon}, \mathbf{\Omega})$ where $\mathbf{\Upsilon} = \epsilon_R^2 \mathbf{I}$ and $\mathbf{\Omega} = 1/\epsilon_R^2 \mathbf{m}\mathbf{m}^H$. From this, the distribution $f_C(\mathbf{C} | \mathbf{H}_s)$ can be acquired by numerically integrating over the linear distribution $f(\alpha)$.

The transmission rate R can be selected such that the mutual information is maximized by optimizing the power allocation for a given outage probability. For a transmission covariance \mathbf{Q} , the outage probability is

$$P_{\text{out}} = \mathbb{P} \left(\log_2 \{ \det [\mathbf{I} + \mathbf{H}_s \mathbf{Q} \mathbf{H}_s^H \mathbf{C}^{-1}] \} < R \right) \quad (10)$$

where the expectation is numerically obtained by integrating over $f_C(\mathbf{C} | \mathbf{H}_s)$.

2) *Joint Tx-Separate Rx*: A transmission mitigating the I/Q interference is used, exploiting the fact that there is a negative correlation between the SINRs of any two eigenbeams. For this, we assume that the joint distribution of SINRs $f_{\Gamma}(\{\gamma_k\})$ is known at the receiver, and a corresponding CQI is sent to the transmitter. Given a transmission covariance, the mutual information $M = \sum_k \log_2(1 + p_k \gamma_k)$ with the linear eigenbeam receiver can be evaluated and a transmission rate is obtained from the mutual information distribution for an outage probability. The maximum rate at a given outage probability is chosen by optimizing the power allocation matrix \mathbf{P} .

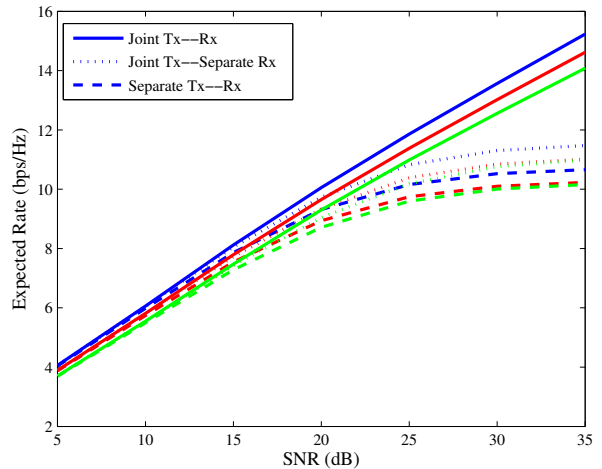


Fig. 4: SNR vs. expected throughput for Joint Tx-Rx, Joint Tx-Separate Rx, and Separate Tx-Rx in block fading downlink.

In a rank-two system with unitary precoding, the joint distribution of SINR is obtained from (9), resulting in

$$f_{\Gamma_1, \Gamma_2}(\gamma_1, \gamma_2 | \mathbf{H}_s) = \frac{\lambda_1 \lambda_2}{(2\gamma_1 \gamma_2)^2} f_{I_1, I_2} \left(\frac{\lambda_1}{2\gamma_1} - \tilde{N}_0, \frac{\lambda_2}{2\gamma_2} - \tilde{N}_0 | \mathbf{H}_s \right) \quad (11)$$

where $\tilde{N}_0 = (1 + \epsilon_R^2)/\gamma_0$ is the I/Q enhanced channel noise power, and $0 \leq \gamma_k \leq \lambda_k/2\tilde{N}_0$. The rate for a given outage probability can be calculated from

$$\begin{aligned} P_{\text{out}} &= \mathbb{P} (\log_2 [1 + \gamma_1] + \log_2 [1 + \gamma_2] < R) \\ &= \int_0^\infty \int_0^{u_2(\gamma_1)} f_{\Gamma_1, \Gamma_2}(\gamma_1, \gamma_2 | \mathbf{H}_s) d\gamma_2 d\gamma_1 \quad (12) \end{aligned}$$

where $u_2(\gamma_1) = \max [2^R/(1 + \gamma_1) - 1, 0]$.

3) *Separate Tx-Rx*: We assume that the marginal SINR distribution $f_{\Gamma}(\gamma_k)$ for each eigenbeam is known to the receiver. The rate on the k th eigenbeam $R_k(P_{\text{out}} | \mathbf{Q}, \mathbf{H}_s)$ is calculated for an outage probability. Individual rates are selected such that the sum of mutual information $M = \sum_k \log_2(1 + p_k \gamma_k)$ is maximized at a given outage probability, where the outage event is considered for each eigenbeam separately. The result of this calculation is sent as a CQI to the transmitter. The mutual information $M_k = \log_2(1 + \gamma_k)$ is distributed according to the marginal distribution of SINRs $f_{\Gamma}(\gamma_k)$.

For rank-two transmissions with unitary precoding, the probability distribution for a given eigenbeam

$$f_{\Gamma}(\gamma | \mathbf{H}_s) = \left| \frac{\lambda}{2\gamma^2} \right| f_I \left(\frac{\lambda}{2\gamma} - \tilde{N}_0 | \mathbf{H}_s \right), \quad 0 \leq \gamma \leq \frac{\lambda}{2\tilde{N}_0} \quad (13)$$

can be obtained from (8) by observing that the SINR of the k th eigenbeam is $\gamma_k = \lambda_k/2(I_k + \tilde{N}_0)$. Consequently, the outage probability for a given transmission rate R can be derived from

$$P_{\text{out}} = \mathbb{P} (\log_2(1 + \gamma) < R) = F_{\Gamma} (2^R - 1) . \quad (14)$$

4) *Performance Comparison for Block Fading*: Fig. 4 shows the expected rate performance as a function of average SNR γ_0 . The three different transmission modes are considered at outage probability [1, 5, 10]% with IRR = 25dB at Tx and Rx. The I/Q interference is rank-one precoded and the interference is accordingly spatially colored. Hence the receiver observes one dimension which does not see any I/Q interference at all. When the receiver performs joint decoding, the information transmitted on this dimension is corrupted only by noise, whereas the information transmitted on the orthogonal dimension is corrupted by the I/Q interference. At high SNR, there is thus one high-SNR dimension left at the receiver. If information is jointly transmitted over the eigenbeams, and jointly decoded, capacity thus grows indefinitely. At high SNR, the capacity does not, however, grow as 2-stream MIMO capacity, but as a single stream capacity. Separate reception results in relatively poor performance at high SNR.

C. Ergodic Fading Channels

In addition to block fading scheduling, as above, a transmission may be scheduled across multiple coherence bandwidths, but still within a coherence time [4], [5]. Due to having a temporally flat channel, it is possible to have perfect CSI at the transmitter. However, in the limit of high frequency selectivity, coding across the frequency domain gives rise to an ergodically fading channel. We assume that both the wanted channel and the interference are ergodic within their respective distributions. That is, a coding block sees all possible channel states and all possible interference states.

The corresponding channel can be formalized as an *ergodic I/Q flashlight channel*. It is characterized by a distribution of the wanted channel \mathbf{H}_s , as well as a the distribution of interference-plus-noise covariance \mathbf{C} . This is an ergodically fading channel with fading caused both by \mathbf{H}_s , as well as by the unknown \mathbf{H}_m and $\overline{\mathbf{W}}$ through \mathbf{C} . Both transmitter and receiver have perfect CSI of \mathbf{H}_s . We assume an instantaneous maximum power constraint satisfied for each channel use.

In ergodically fading channels, link adaptation based on known statistics of the SINR distribution has been discussed in [38], [39]. Here we assume perfect knowledge of the pertinent distributions. The distribution of received SINR can be computed from the distribution of the eigenvalues of the wanted channel and the distribution of the induced interference at a given SNR while precoder selection is done on instantaneous channel gains. We again consider the Tx-Rx strategies of Section II-B. However, due to ergodicity, Joint Tx-Separate Rx gives the same rate as a Separate Tx-Rx.

1) *Joint Tx-Rx*: Here, the receiver knows the realization of \mathbf{C} for all subcarriers used, as well as the statistic $f_{\mathbf{C}}(\mathbf{C})$. For link adaptation, the receiver constructs a CQI from the perfectly known distributions of the desired channel and the interference covariance. The capacity reaching transmission covariance $\mathbf{Q}(\mathbf{H}_s)$ maximizes the mutual information

$$R = \mathbb{E}_{\mathbf{H}_s, \mathbf{C}} \left\{ \log_2 \left\{ \det \left[\mathbf{I} + \mathbf{H}_s \mathbf{Q} \mathbf{H}_s^H \mathbf{C}^{-1} \right] \right\} \right\} \quad (15)$$

2) *Separate Tx-Rx*: The receiver is aware of the marginal SINR distributions $f_{\Gamma}(\gamma_k)$, and constructs a CQI based on this, made available to the transmitter. The expected rate is

$$R = \mathbb{E}_{\gamma_k} \left\{ \sum_k \log_2 (1 + p_k \gamma_k) \right\} . \quad (16)$$

The rate is maximized over the power allocations p_k .

The statistics of SINR can be drawn from the distributions of channel eigenvalues and the interference. The eigenvalue distribution can be obtained from [40]. For 2×2 MIMO, the eigenvalue distributions are $f_{\Lambda}(\lambda_1) = (\lambda_1^2 - 2\lambda_1 + 2)e^{-\lambda_1} - 2e^{-2\lambda_1}$ and $f_{\Lambda}(\lambda_2) = 2e^{-2\lambda_2}$, $\lambda_1 > \lambda_2$. For a given channel \mathbf{H}_s , the SINR distribution of the k th eigenbeam is given by (13). Therefore, the SINR distribution for the ergodic channel can be derived from

$$f_{\Gamma}(\gamma) = \int_0^{\infty} f_{\Gamma}(\gamma | \mathbf{H}_s) f_{\Lambda}(\lambda) d\lambda . \quad (17)$$

The eigenvalue distributions can be represented as algebraic sums of terms of the form $\lambda^p e^{-q\lambda}$, $p, q > 0$. The SINR distribution function $f_{p,q}(\gamma)$ for a RV λ distributed as $\lambda^p e^{-q\lambda}$ is given by

$$f_{p,q}(\gamma) = \sum_{m=0}^{\infty} \sum_{n=0}^{\infty} \frac{I_0^m e^{-\frac{\tilde{N}_0}{\tilde{\epsilon}_R^2}}}{(2\gamma)^{m+1}} \left(\frac{\epsilon_T^{m+n}}{\epsilon_R^{2m+n+1}} \right)^2 \tilde{U}(a, b, z)_{p,q} \quad (18)$$

where $\tilde{U}(a, b, z)_{p,q}$ is $\prod_{r=1}^p (m+n+r+1) \Gamma[m+1]$ times the Confluent Hypergeometric function,² $a = m+n+p+2$, $b = m+a+1$, and $z = q + \frac{1+2\gamma\epsilon_T^2}{2\gamma\epsilon_R^2}$. The distribution of the weakest eigenvalue thus is

$$f_{\Gamma}(\gamma_2) = 2f_{1,2}(\gamma) , \quad (19)$$

and the distribution of the strongest eigenvalue is

$$f_{\Gamma}(\gamma_1) = \sum_{k=0}^1 (2-k) f_{k,1}(\gamma) - 2f_{k,2-k}(\gamma) . \quad (20)$$

Knowing the marginal and joint SINR distributions, average transmission rates can be derived from (16) for separate reception.

3) *Performance Comparison for Ergodic Fading*: Fig. 5 shows the average rate performance for a given SNR γ_0 at IRR = 25dB at Tx and Rx. The knowledge of I/Q interference covariance at the transmitter compensates I/Q interference automatically by transmitting information on the eigen directions that do not suffer from I/Q interference. This leads to infinitely increasing ergodic rate behavior. However, the lacking knowledge of I/Q interference covariance, or of the correlation between the SINRs, degrades the rate performance in Separate Tx-Rx. At high SNR, I/Q interference dominates and rate saturates.

²The Confluent Hypergeometric function can be written in integral form as $U(a, b, z) = \frac{1}{\Gamma[a]} \int_0^1 e^{-zt} t^{a-1} (1+t)^{b-a-1} dt$, $\Re\{a\} > 0$

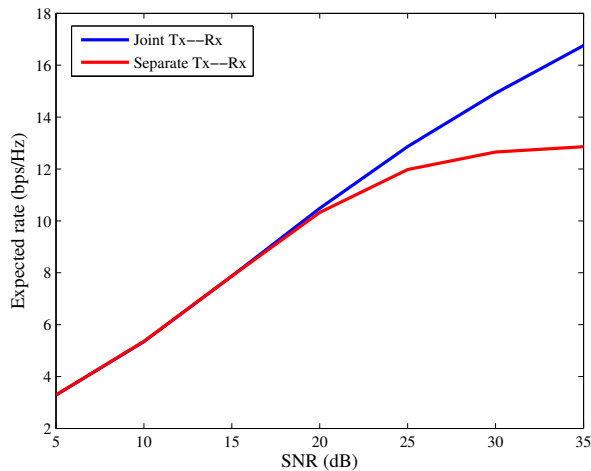


Fig. 5: SNR vs. average rate for ergodic fading downlink. Modes Joint Tx-Rx and Separate Tx-Rx. I/Q imbalance IRR = 25dB at transmitter and receivers.

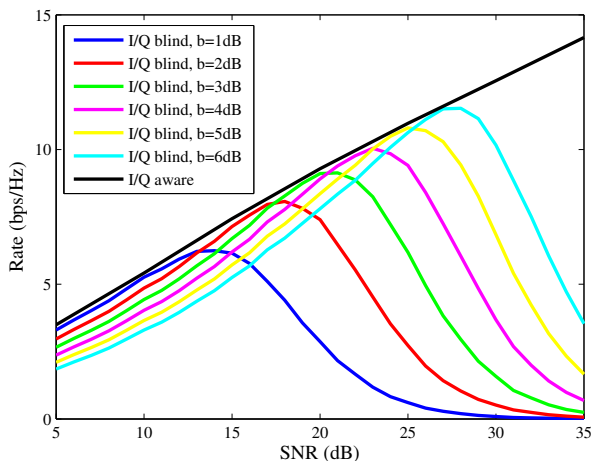


Fig. 6: SNR vs. expected rate for block fading downlink, with Joint Tx-Rx. I/Q imbalance IRR = 25dB at transmitter and receivers, and variable back-off b dB.

V. I/Q-BLIND VS. I/Q-AWARE LINK ADAPTATION

When the form of the SINR distribution is not known at the receiver, accurate optimization of the transmission method is not possible. To compare I/Q aware to I/Q blind link adaptation, we apply open loop link adaptation [41]. Given an SINR estimate $\hat{\gamma}$ characterizing the channel, a transmission rate is conservatively selected according to a backed-off SINR $\tilde{\gamma} = \frac{\hat{\gamma}}{b}$, where b is the blind back-off value. Here, we consider a scenario, where from a known pilot transmission, the receiver estimates the average SNR: $\hat{\gamma} = \gamma_0$. In block fading, channel gains are known to the receiver and in ergodic fading, statistical information of the eigenvalues are known.

Transmission and reception can be done jointly or separately as in I/Q aware transmission. For ergodic I/Q flashlight channels, a suitably chosen blind back-off performs nearly indistinguishably from the I/Q aware schemes in Fig. 5. For block

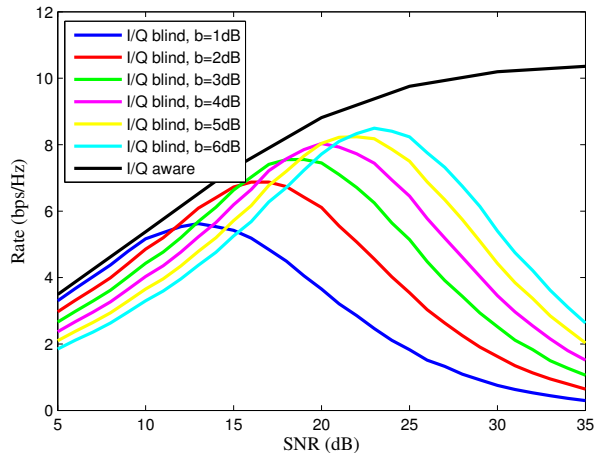


Fig. 7: SNR vs. the expected rate for block fading downlink with Separate Tx-Rx. I/Q imbalance IRR = 25dB at transmitter and receivers, and variable back-off b dB.

fading I/Q flashlight channels, the situation is more nuanced. For I/Q ignorant link adaptation for separate transmission, we assume that the same b is used for all eigenbeams. In joint transmission, the transmitter sets a rate \hat{R} to comply with the mutual information $\hat{M} = \log_2 \left\{ \det \left[\mathbf{I} + \mathbf{H}_s \hat{\mathbf{Q}} \mathbf{H}_s^H \hat{\mathbf{C}}^{-1} \right] \right\}$, where the transmit covariance $\hat{\mathbf{Q}} = \mathbf{W} \mathbf{P} \mathbf{W}^H$ has a power allocation matrix \mathbf{P} obtained by water filling. With a back-off, the predicted interference covariance $\hat{\mathbf{C}} = \tilde{\gamma} \mathbf{I}$ is used. To assess performance, the outage probability for joint reception can be computed from the realized interference covariance \mathbf{C} , and the expected rate can be calculated by averaging over \mathbf{H}_s and \mathbf{C} . In separate reception, the receiver experiences outage depending on the realization of the SINRs for the eigenbeams, and the corresponding mutual information $M = \sum_k \log_2(1 + p_k \gamma_k)$ supported by the realized channel. An expected rate may then be calculated, averaging over \mathbf{H}_s and $f_{\Gamma}(\{\gamma_k\})$.

For Separate Tx-Rx, the transmitter applies the individual rates $\hat{R}_k = \log_2(1 + p_k \tilde{\gamma}_k)$ for each eigenbeam. The receiver experiences outage according to the marginal distributions $f_{\Gamma}(\gamma_k)$ on the eigenbeams and an expected rate per eigenbeam is obtained. The expected rate of the system is the sum of the per beam expected rates.

Figures 6 and 7 illustrate the rate performance with back-off against SNR for Joint Tx-Rx and Separate Tx-Rx. The performance Joint Tx-Separate Rx is between these two. Simulation is carried out for back-off in the range $b = 1 - 6$ dB at I/Q imbalance level IRR = 25dB. The maximum expected rate achieved by I/Q aware link adaptation is plotted in the same figure. For Joint Tx-Rx, the joint transmission and optimum receiver are capable of mitigating I/Q interference, and an SNR-dependent back-off value would be sufficient to nearly reach the performance of I/Q aware link adaptation. In separate transmission, an SNR based back-off technique is unable to track the maximum expected rates as the same blind back off value is used for both streams. To reach the performance of I/Q aware back-off, separate back-off values are needed for

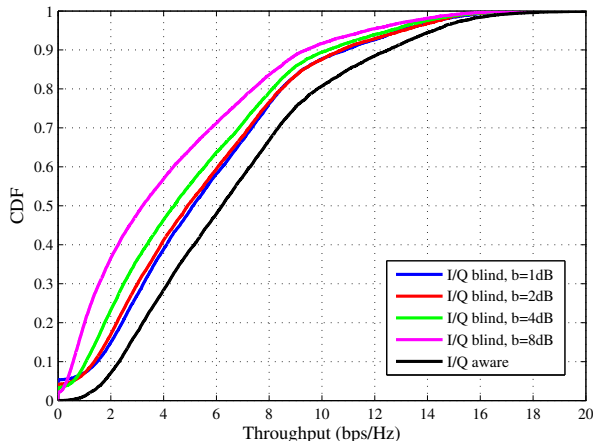


Fig. 8: Cumulative rate distribution with I/Q aware and ignorant downlink transmission. Simulations are carried out for $b = [1, 2, 4, 8]$ dB at IRR = 25dB I/Q imbalance level at the transmitter and the receivers.

the eigenbeams, which depend both on the SNR, and the beam eigenvalue.

VI. SYSTEM SIMULATION

To get an understanding of the effect of I/Q aware and non-aware link adaptation in a practical cellular system with co-channel interference, system simulations have to be performed. Here, we consider a typical cellular network deployment implemented according to the system level parameters given in the Table A.2.1.1-3 [37]. The simulated scenario is a micro-cellular network with omni-directional transmissions, which has been used for MIMO evaluations in LTE studies.

In the modeled system, we assume that half of the terminals have one antenna, and the other half two antennas, whereas all base stations have two antennas. Thus for a given transmission on the subcarrier of interest, the receiver is experiencing I/Q interference either from single or dual stream mirror subcarrier transmission with an equal probability. In addition to the co-channel interference, both the transmitter and receivers suffer from frequency flat I/Q imbalance. Separate Tx-Rx is assumed, and equal power allocation is assumed on both subcarrier and mirror carrier. It is assumed that link adaptation is based on knowledge of the rank of the mirror carrier transmission.

Fig. 8 depicts the distribution of the rates achieved by the users for I/Q aware and non-aware link adaptation. The I/Q aware transmission achieves best transmission rates. The I/Q non-aware blind back-off selection performs well at low back-off values. However, for small back-off values, mispredictions of SINR cause many users to be in an outage. For example, for 1dB back-off, 5% of the users are in an outage. When we increase the back-off the average throughput of the system drops while the outage probability decreases.

VII. DISCUSSION

We have assumed perfect CSI at the transmitter, as well as error-free channel estimates at the receiver, and we have

concentrated on the effects of MIMO-I/Q interference on mispredictions of CQI. Both time and frequency selectivity of wireless channels, however, affect performance in two ways, by adding interference at the receiver, and by limiting the accuracy of CQI.

The effects on performance of added interference caused by time and frequency dispersion can largely be taken care of by proper system parametrization. In an OFDM system, perfect removal of ISI caused by time dispersion is possible as long as the excess delay τ_E of the channel is shorter than the CP duration τ_{CP} . Similarly, Inter-Carrier Interference (ICI) caused by frequency dispersion is negligible, as long as the Doppler spread f_D is much less than the subcarrier spacing. For LTE [37], the short CP is $\tau_{CP} = 4.7\mu s$, whereas the subcarrier spacing is $f_{subc} = 15kHz$. With a 2GHz carrier frequency, we have $f_D/f_{subc} \approx 2.5 * 10^{-4}v$, where v is the velocity in units of km/h. Thus with velocities up to tens of km/h, ICI is insignificant, and in environments with path length differences less than 1.4 km, the ISI and ICI caused by dispersion effects would not be an issue in LTE.

For link-adaptation, the dual selectivity effects, however, are relevant. Due to time selectivity, the channel quality will change between the time of estimation and time of data transmission [26]. Furthermore, due to frequency selectivity, the channel estimated from certain pilot subcarriers may not represent the channel in other subcarriers. This leads to CQI errors. For Rayleigh fading channels, the difference between the realized and measured channels due to channel selectivity can be modeled as [26], [29]

$$h = \rho \hat{h} + \sqrt{1 - \rho^2} \tilde{h}. \quad (21)$$

Here, h is the channel realized under transmission, \hat{h} is the measured channel, and ρ is the correlation coefficient. The estimation error \tilde{h} is an independent sample from the same complex channel distribution as h and \hat{h} . The correlation coefficient is drawn from Jakes' model when considering time selectivity, and from [42, Eq. 19] when corresponding frequency selectivity.

Conditioned on \hat{h} , the SINR variability due to imperfect CQI can be modelled by the relative CQI difference $\delta = |h/\hat{h}|^2$. It is Rician power distributed with parameters ρ and $(1 - \rho^2)/\gamma$, where $\gamma = |\hat{h}|^2$ [29]. It is notable that the relative strength of the random component decreases with γ , as noted in [26] for generic prediction processes. Here, we are interested in distributions of prediction errors for Rayleigh channels with an average power γ_0 , and thus integrate over an exponentially distributed γ . As a result we get

$$f_{\Delta}(\delta|\gamma_0) = \frac{1}{2} \frac{(\delta + c_+)(c_+ - c_-)}{((\delta + c_-)^2 + c_+^2 - c_-^2)^{3/2}} \quad (22)$$

where $c_{\pm} = ((\gamma_0 \mp 2)\rho^2 \pm 2)/\gamma_0$.

The characteristics of the CQI variation δ induced by time and frequency selectivity in Rayleigh fading can thus be compared to the CQI variation induced by the MIMO-I/Q flashlight effect. For a block fading channel with separate transmission, we have the SINR distribution (13), from which a distribution of δ can be derived. In Fig. 9 we compare

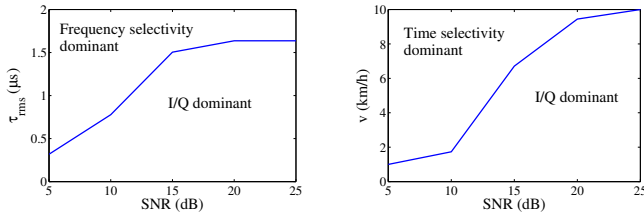


Fig. 9: Dominant source of CQI variability. Left: Frequency selectivity vs. MIMO-I/Q interference. Right: time selectivity vs. MIMO-I/Q interference

CQI variability caused by time selectivity and frequency selectivity to the variability caused by the I/Q flashlight effect. When modeling time selectivity, we assume a 2 GHz carrier frequency, and 4ms delay between the CQI estimate, and the actual transmission. When modeling frequency selectivity, we assume perfectly known channel at the pilot carriers, and base the CQI estimate on these. Modeling an LTE system, we assume that one pilot subcarrier is assumed to directly give the channel estimate for three subcarriers. The realized channel quality is modeled by the average of all subcarrier channel powers, and ρ is calculated according to [42]. Frequency selective fading channels with six equidistant delay taps were modeled, with excess delays up to the LTE CP duration. The corresponding Root-Mean-Square delays τ_{rms} are up to 1.8 μs .

We compute the variance of the distribution of δ for different average SINRs γ_0 , and for different velocity v and τ_{rms} . In the low-speed & high SINR region, the I/Q flashlight effect causes more variability than time selectivity. Similarly, for short τ_{rms} and high SINR, the I/Q flashlight effect dominates over the CQI errors given by frequency selectivity.

The CQI errors caused by the I/Q flashlight effect should also be compared to those created by other RF impairments. These will not have a similar dramatically varying effect as the I/Q interference has, however. ICI caused by phase noise and carrier frequency offset is localized in the frequency, and thus in an OFDMA system with resource blocks consisting of multiple subcarriers, such as LTE, the largest effects will be within the resource block. Nonlinearity noise from the power amplifier spreads distributions evenly over the full transmission band, and is known to be almost Gaussian in OFDM(A).

VIII. CONCLUSION

The impact of mirror subcarrier precoder selection on the transmissions in MIMO-OFDMA systems was investigated. If the transmission on the mirror subcarrier is spatially colored, the I/Q interference experienced at the subcarrier of interest becomes dependent on the link adaptation and scheduling decisions on the mirror carrier. This causes fading due to non-controlled variations in the signal quality. When the source of the interference, and its statistics are known, an I/Q aware transmitter may select an optimum transmission method. Here we investigated link adaptation in a situation where the transmission on the mirror subcarrier is not full rank, and the I/Q interference correspondingly becomes spatially colored. Block and ergodic fading channel models were considered.

In ergodic fading, link adaptation may be performed based on statistical knowledge of the channel and interference. We found that the gains from I/Q awareness are limited—an I/Q ignorant transmitter slightly underestimates the rate that the channel may support.

In a block fading channel, link adaptation is based on the statistics of the I/Q interference, and the instantaneous channel strength of the wanted transmission. Expected throughput may be maximized subject to outage caused by I/Q interference variations. The performance of an I/Q aware transmission was found to outperform an I/Q ignorant transmission based on an SINR-independent blind back-off. A codeword-specific SINR-dependent back-off scheme would perform almost as well as I/Q-aware link adaptation.

The analysis has been based on assumptions on ideal infinite granularity link adaptation, and perfect CSI. We have argued that at high SINR, pedestrian speeds, and short delay spreads, which would be predominant in small cell networks, the I/Q interference is the dominant source of CQI errors. With imperfect CSI, caused e.g. by time selectivity or channel estimation errors, the distributions used for link adaptation would change. In addition to the I/Q-effect, one should jointly consider at the distributions caused by the other sources of error [24]–[26]. Also, if power allocation across beams would be applied, instead of unitary precoding, the distribution of I/Q interference would widen. The overall CQI error distribution would be the convolution of the CQI error distributions of all independent sources of error. However, the link adaptation principle of this paper would hold, and I/Q aware link adaptation would outperform I/Q blind.

ACKNOWLEDGMENT

This work has been supported by the Academy of Finland (grant 254299). We thank the anonymous reviewers for their insightful and constructive comments.

REFERENCES

- [1] 3GPP; TSG RAN, “Evolved universal terrestrial radio access (E-UTRA) and evolved universal terrestrial radio access network (E-UTRAN); overall description; Stage 2 (Release 8),” TS 36.300, Sep. 2008.
- [2] H. Yaghoobi, “Scalable OFDMA physical layer in IEEE 802.16 wireless man,” *Intel Technology J.*, vol. 8, pp. 201–212, Aug. 2004.
- [3] E. S. Lo & al., “Adaptive resource allocation and capacity comparison of downlink multiuser MIMO-MC-CDMA and MIMO-OFDMA,” *IEEE Trans. Wireless Commun.*, vol. 6, no. 3, pp. 1083–1093, May 2007.
- [4] H. Zhu and J. Wang, “Chunk-based resource allocation in OFDMA systems - Part I: Chunk allocation,” *IEEE Trans. Commun.*, vol. 57, no. 9, pp. 2734–2744, Sep. 2009.
- [5] —, “Chunk-based resource allocation in OFDMA systems - Part II: Joint chunk, power and bit allocation,” *IEEE Trans. Commun.*, vol. 60, no. 2, pp. 499–509, Sep. 2012.
- [6] S. T. Chung and A. J. Goldsmith, “Degrees of freedom in adaptive modulation: A unified view,” *IEEE Trans. Commun.*, vol. 49, no. 9, pp. 1561–1571, Sep. 2001.
- [7] S. Schwarz, C. Mehlh r, and M. Rupp, “Calculation of the spatial preprocessing and link adaption feedback for 3GPP UMTS/LTE,” in *Proc. IEEE 6th Conference on Wireless Advanced (WiAD)*, Jun. 2010, pp. 1–6.
- [8] P.E. Mogensen & al., “5G small cell optimized radio design,” in *Proc. IEEE Conf. on Global Telecommunications (GLOBECOM)*, Dec. 2013, pp. 1–6.
- [9] A. Tarighat, R. Bagheri, and A. H. Sayed, “Compensation schemes and performance analysis of IQ imbalances in OFDM receivers,” *IEEE Trans. Signal Process.*, vol. 53, no. 8, pp. 3257–3268, Aug. 2005.

- [10] M. Windisch and G. Fettweis, "Standard-independent I/Q imbalance compensation in OFDM direct-conversion receivers," in *Proc. IEEE Internat. OFDM Workshop*, vol. 53, no. 9, Sep. 2004, pp. 57–61.
- [11] P. Capozio, P. Pai, E. Vizzi, and G. Dacosta, "A novel adaptive technique for digital I/Q imbalance compensation in OFDM receivers," in *Proc. IEEE Internat. Conf. on Acoustics, Speech, and Sign. Proc. (ICASSP)*, Mar. 2005, pp. 817–820.
- [12] K. Sung and C. Chao, "Estimation and compensation of I/Q imbalance in OFDM direct-conversion receivers," *IEEE J. Sel. Topics Signal Process.*, vol. 3, no. 3, pp. 438–453, Jun. 2009.
- [13] S. Bassam, S. Boumaiza, and F. M. Ghannouchi, "Block-wise estimation of and compensation for I/Q imbalance in direct-conversion transmitters," *IEEE Trans. Signal Process.*, vol. 57, no. 12, pp. 4970–4973, Dec. 2009.
- [14] L. Anttila, M. Valkama, and M. Renfors, "Gradient-based blind iterative techniques for I/Q imbalance compensation in digital radio receivers," in *Proc. IEEE Internat. Workshop on Sign. Proc. Advances in Wireless Commun. (SPAWC)*, Jun. 2007, pp. 1–5.
- [15] C.-P. Yen, Y. Tsai, G. Zhang, and R. Olesen, "Blind estimation and compensation of frequency-flat I/Q imbalance using cyclostationarity," in *Proc. IEEE 68th Vehicular technology Conf. (VTC)*, Sep. 2008, pp. 1–5.
- [16] H. Lin and K. Yamashita, "Time domain blind I/Q imbalance compensation based on real-valued filter," *IEEE Trans. Wireless Commun.*, vol. 11, no. 12, pp. 4342–4350, Dec. 2012.
- [17] B. Narasimhan, S. Narayanan, N. Al-Dhahir, and H. Minn, "Reduced-complexity baseband compensation of joint Tx/Rx I/Q imbalance in mobile MIMO-OFDM," *IEEE Trans. Commun.*, vol. 9, no. 5, pp. 1720–1728, May 2010.
- [18] J. Qi and S. Aissa, "Analysis and compensation of I/Q imbalance in MIMO transmit-receive diversity systems," *IEEE Trans. Commun.*, vol. 58, no. 5, pp. 1546–1556, May 2010.
- [19] H. Mahmoud, H. Arslan, M. Ozdemir, and F. Retnasothie, "IQ imbalance correction for OFDMA uplink systems," in *Proc. IEEE Internat. Conf. on Commun. (ICC)*, Jun. 2009, pp. 1–5.
- [20] Y. Yoshioda, K. Hayashi, H. Sakai, and W. Bocquet, "Analysis and compensation of transmitter IQ imbalances in OFDMA and SC-FDMA systems," *IEEE Trans. Signal Process.*, vol. 57, no. 8, pp. 3119–3129, Aug. 2009.
- [21] B. Maham and O. Tirkkonen, "Impact of transceiver I/Q imbalance on transmit diversity of beamforming OFDM systems," *IEEE Trans. Commun.*, vol. 60, no. 3, pp. 643–648, Mar. 2012.
- [22] O. Ozdemir, R. Hamila, and N. Al-Dhahir, "I/Q imbalance in multiple beamforming OFDM transceivers: SINR analysis and digital baseband compensation," *IEEE Trans. Commun.*, vol. PP, no. 99, pp. 1–12, Oct. 2013.
- [23] U. Oruthota and O. Tirkkonen, "I/Q imbalance compensation in precoded MIMO-OFDMA systems," in *Proc. Internat. Symp. on Wireless Personal Multimedia Commun. (WPMC)*, Sep. 2012, pp. 291–295.
- [24] A. J. Goldsmith and S. G. Chua, "Variable-rate variable-power MQAM for fading channels," *IEEE Trans. Commun.*, vol. 45, no. 10, pp. 1218–1230, Oct. 1997.
- [25] D. L. Goeckel, "Adaptive coding for time-varying channels using outdated fading estimates," *IEEE Trans. Commun.*, vol. 47, no. 6, pp. 844–855, Jun. 1999.
- [26] S. Falahati, A. Svensson, T. Ekman, and M. Sternad, "Adaptive modulation systems for predicted wireless channels," *IEEE Trans. Commun.*, vol. 52, no. 2, pp. 307–316, Mar. 2004.
- [27] A. Osseiran and A. Logothetis, "Closed loop transmit diversity in WCDMA HS-DSCH," in *Proc. IEEE Vehicular Technology Conf. (VTC)*, Jun. 2005, pp. 349–353.
- [28] J. Kurjenniemi, T. Nihtilä, E. Virtej, and T. Ristaniemi, "On the effect of reduced interference predictability to the HSDPA network performance with closed loop transmit diversity," in *Proc. Internat. Symp. on Wireless Personal Multimedia Commun. (WPMC)*, Sep. 2006, pp. 864–868.
- [29] C. H. Yu and O. Tirkkonen, "Rate adaptation of AMC/HARQ systems with CQI errors," in *Proc. IEEE 71st Vehicular Technology Conf. (VTC)*, May 2010, pp. 1–5.
- [30] S. Krone and G. Fettweis, "Capacity analysis for OFDM systems with transceiver i/q imbalance," in *Proc. IEEE Conf. on Global Telecommunications (GLOBECOM)*, Nov. 2008, pp. 1–6.
- [31] B. Maham and O. Tirkkonen, "Transmit antenna selection OFDM systems with transceiver I/Q imbalance," *IEEE Trans. Veh. Technol.*, vol. 61, no. 2, pp. 865–871, Feb. 2012.
- [32] B. Razavi, "Design considerations for direct-conversion receivers," *IEEE Trans. Circuits Syst. II*, vol. 44, pp. 428–435, Jun. 1997.
- [33] M. Cao and H. Ge, "GLCP OFDM systems with I/Q imbalance," *IEEE Commun. Lett.*, vol. 13, no. 4, pp. 230–232, Apr. 2009.
- [34] U. Oruthota, O. Tirkkonen, and N. Ermolova, "Analysis of space-frequency coded OFDM with I/Q imbalance," in *Proc. IEEE Internat. Conf. Ultra-modern Commun. (ICUMT)*, Oct. 2010, pp. 275–280.
- [35] T. C. W. Schenk, P. F. M. Smulders, and E. R. Fledderus, "Estimation and compensation of frequency selective TX/RX IQ imbalance in MIMO OFDM systems," in *Proc. IEEE Internat. Conf. on Commun. (ICC)*, Jun. 2006, pp. 251–256.
- [36] Y. Egashira, Y. Tanabe, and K. Sato, "A novel IQ imbalance compensation method with pilot-signals for OFDM system," in *Proc. IEEE Vehicular Technology Conf. (VTC)*, Sep. 2006, pp. 1–5.
- [37] 3GPP; TSG RAN, "Physical layer aspects for evolved universal terrestrial radio access (UTRA) (release 7)," TR 25.814 v7.1.0, Sep. 2006.
- [38] M. Lampe, V. Rohling, and W. Zirwas, "Misunderstandings about link adaptation for frequency selective fading channels," in *Proc. IEEE 13th International Symposium on Personal, Indoor and Mobile Radio Communications (PIMRC)*, Sep. 2002, pp. 710–714.
- [39] S. Catreux, V. Erceg, D. Gesbert, and R. Heath, "Adaptive modulation and MIMO coding for broadband wireless data networks," *IEEE Commun. Mag.*, vol. 40, no. 6, pp. 108–115, Jun. 2002.
- [40] A. Zanella and M. Chiani, "The PDF of the l 'th largest eigenvalue of central Wishart matrices and its application to the performance analysis of MIMO systems," in *Proc. IEEE Global Telecommunications Conf. (GLOBECOM)*, Nov. 2008, pp. 1–6.
- [41] M. Nakamura, Y. Awad, and S. Vadgama, "Adaptive control of link adaptation for high speed downlink packet access (HSDPA)," in *Proc. Internat. Symp. on Wireless Personal Multimedia Commun. (WPMC)*, Oct. 2002, pp. 382–386.
- [42] Q. T. Zhang and S. Song, "Exact expression for the coherence bandwidth of Rayleigh fading channels," *IEEE Trans. Commun.*, vol. 55, no. 7, pp. 1296–1299, Jul. 2007.